Effect of Face Mask Leaks on Inhaled Corticosteroid Delivery to Infants

by

Nicholas B. Carrigy

A thesis submitted in partial fulfillment of the requirements for the degree of

Master of Science

Department of Mechanical Engineering
University of Alberta

ABSTRACT

Infant face and throat replicas are used in research laboratories to compare the effectiveness of different valved holding chamber and face mask designs. The use of soft face models is thought to provide a better representation of mask dead volume and face mask seal than hard face models. However, a comparison of mask dead volume, face mask seal, and lung dose for soft versus hard face models is lacking.

This study compares mask dead volume, face mask seal, and lung dose for hard ABS, soft silicone, and very soft polyurethane facial materials at two clinically relevant applied forces: 1.5 lb and 3.5 lb. Mask dead volume is quantified using water displacement. Face mask seal is quantified using flow rate measurement. The lung dose of beclomethasone dipropionate delivered via a Qvar® pressurized metered dose inhaler with AeroChamber Plus Flow-Vu™® Valved Holding Chamber and Small Mask, defined as that which passes through the nasal airways of an idealized infant model, is quantified using a bias tidal flow system with a filter. A mathematical model is used to predict lung dose based on experimental results of mask dead volume and flow rate through the valved holding chamber.

This study shows that a greater lung dose is obtained using soft face models as compared to hard face models, with a greater difference at 1.5 lb than 3.5 lb. Face mask leakage led to decreased dose consistency and therefore a sealant should be applied when measuring lung dose with a hard ABS or soft silicone face model at 1.5 lb of applied force or less. Parametric analysis with the mathematical model showed that differences in face mask seal between face models were more predictive of lung dose than differences in mask dead volume.

PREFACE

This thesis is contains material from the following publications:

Carrigy NB, O'Reilly C, Schmitt J, Noga M, and Finlay WH: Effect of Facial Material Softness and Applied Force on Face Mask Dead Volume, Face Mask Seal, and Inhaled Corticosteroid Delivery Through an Idealized Infant Replica. *Journal of Aerosol Medicine and Pulmonary Drug Delivery.* Accepted September 6, 2013. doi:10.1089/jamp.2013.1087.

Carrigy NB, Ruzycki CA, Golshahi L, and Finlay WH: Pediatric *In Vitro* and *In Silico* Models of Deposition via Oral and Nasal Inhalation. *Journal of Aerosol Medicine and Pulmonary Drug Delivery*. 2014;27(3):149-169.

Carrigy NB, O'Reilly C, Schmitt J, Noga M, and Finlay WH: Quantification of Inhaled Beclomethasone Dipropionate Delivery, Face Mask Seal, and Mask Dead Volume for Different Push-on Forces and Facial Materials with an Idealized Infant Replica. Abstract and poster. *Respiratory Drug Delivery 2014*. May 4-8 2014, Fajardo, Puerto Rico.

DEDICATION

To Laura Dazé

ACKNOWLEDGEMENTS

I would like to thank my M.Sc. advisor Professor Warren H. Finlay for the valuable feedback he has provided to me throughout this degree. His supervision of the work leading to this thesis is greatly appreciated. I would like to thank him particularly for allowing me to take nearly a month off research to volunteer in Africa near the end of this degree.

I would like to thank Helena Orszanska for providing me with valuable feedback throughout the experimental design process and for timely filter measurement results. James Schmitt's expertise in rapid prototyping was invaluable for the fabrication of the face models. Rick Bubenko and the other machine shop technicians kindly trained me on the use of machine shop equipment. Rick Conrad designed the in-house amplifiers used in this study and graciously dropped what he was doing on multiple occasions to help me fix the load cell system when it malfunctioned.

Conor Ruzycki provided me with useful tips regarding experimental measurements and was always willing to troubleshoot problems with me, and also helped me with course work. His efforts towards writing our review paper on pediatric deposition models, as well as those of Laleh Golshahi, are highly appreciated. My labmates Azadeh Akhavan Taheri Borojeni, Mehdi Azhdarzadeh, and Farzin Molaghasem Shemirani graciously provided answers to any questions I had, and allowed me to borrow their equipment and lab-space on numerous occasions.

I am blessed to have a wonderful family who supported me and helped me with whatever I needed throughout this degree. Thank you to Colin, Janice, and Alec. My grandfather Maurice, a researcher during his entire career, has been an excellent example for me. My grandmother Shirley has provided moral support. My girlfriend Megan Germsheid has

been a source of happiness and support for me and I look forward to what the future may bring for us.

During the latter portion of my degree where my research shifted to computational anatomy modeling for the purposes of obstructive sleep apnea simulations, I was fortunate enough to meet the research and design department staff at Zephyr Sleep Technologies, with whom I enjoyed having informative talks at our meetings. Dr. John Remmers, Ali Zareian, Zbigniew Topor, and Joshua Grosse were very helpful despite their busy work schedules. Andrew Martin has provided helpful feedback with regards to the sleep apnea project and Jason Carey has been kind enough to offer me desk space to work in his lab, a computer, and a Simpleware license.

I gratefully acknowledge the University of Alberta Faculty of Graduate Studies and Research for providing me with two Queen Elizabeth II Graduate Scholarships during this degree program, and also the Alberta Scholarship Programs for a Graduate Student Scholarship. The Natural Sciences and Engineering Research Council of Canada and the Canadian Institutes of Health Research are also acknowledged for providing grants to cover the equipment and services used in this study, as well as a part of my research assistantship salary.

Nicholas Benjamin Carrigy

June 11, 2014

Sherwood Park, Alberta, Canada

TABLE OF CONTENTS

TABLE OF CONTENTS

LIST OF TABLES

LIST OF FIGURES

LIST OF FIGURES

LIST OF SYMBOLS

$T_{1/2}$ – aerosol half-life in the valved holding chamber

V_a – aerosol volume inhaled

V_L – air leak volume inhaled

C_a – concentration of inhaled aerosol in the first breath

DD – delivered dose, ex-actuator

η – extrathoracic deposition fraction

MDV – face mask dead volume

a – face mask dead volume correction factor

Q_{throat} – flow rate through throat

Q_{VHC} – flow rate through valved holding chamber

ED – fraction of delivered dose initially available for inhalation from valved holding chamber

t_i – inspiration time

LD – lung dose in n respiratory cycles

LD_1 – lung dose for the first breath

LD_i – lung dose for the i^{th} respiratory cycle

V_{NA} – nasal airway volume

LIST OF SYMBOLS

b – nasal airway volume correction factor

n – number of respiratory cycles

RF – remaining fraction of aerosol in the valved holding chamber after one breath

f – respiratory cycle frequency

i – respiratory cycle index

V_t – tidal volume

n – total number of respiratory cycles

V_{VHC} – valved holding chamber volume

LIST OF ABBREVIATIONS

BDP – beclomethasone dipropionate

CI – confidence interval

CT – computed tomography

MMAD – mass median aerodynamic diameter

pMDI – pressurized metered dose inhaler

SAINT – Sophia Anatomical Infant Nose-Throat

UV – ultraviolet-visible

VHC – valved holding chamber

CHAPTER 1: INTRODUCTION

1.1 Inhaled Corticosteroid Delivery to Infants

Infants are unable to perform the inhalation technique required for optimal use of a pressurized metered dose inhaler (pMDI).[1] Consequently, a valved holding chamber (VHC) and face mask is commonly attached to a pMDI to treat asthmatic infants.[1-2] Figure 1 shows a caregiver applying a pMDI with VHC and face mask to an infant's face.

Figure 1: Caregiver applying a VHC and face mask to an infant's face.[3] Reprinted with permission from Forest Laboratories, Inc.

This delivery method allows the infant to inhale the aerosolized medication tidally while limiting extrathoracic deposition and associated side effects. *In vivo*[4] and *in vitro*[5-6] studies have shown that this delivery method requires a tight face mask seal to ensure effective aerosol delivery to the lungs. A tight face mask seal ensures that the inspiration valve opens and the inhaled aerosol is not diluted by ambient air. Without an adequate face mask seal, longer administration times may be required and the pharmaceutical aerosol may settle to the bottom

of the VHC instead of reaching the lungs. Unfortunately, a lack of cooperation from the infant can create difficulties with maintaining an adequate face mask seal.[7-10] When infants cry or scream increased peak inspiratory flow rates can result which may lead to increased extrathoracic deposition.[7] Consequently, the caregiver might apply too little force to the VHC to avoid upsetting the infant. To put the infant at ease during the aerosol administration process diversions such as toys, videos, or making a game of it have been suggested,[1,11] as has using a pacifier in the face mask.[12-13] Since infants have low tidal volumes, another requirement for effective drug delivery is minimal dead volume within the face mask.[13-14]

1.2 Literature Review – pMDI VHC Face Mask *In Vitro* Studies

Everard *et al*.[14] showed that minimal dead volume between the inhalation valve of a holding chamber and the patient is essential for effective drug delivery to infants due to their low tidal volumes. Therefore, *in vitro* water displacement techniques have been used to determine face mask dead volume for different applied forces.[15-16] Using a flat plate with a hole to represent the mouth, Chavez *et al.*[17] found that decreasing mask dead volume, increasing tidal volume, and increasing respiratory rate all increased inhaled mass of albuterol. Everard *et al*.[14] showed that VHCs used with infants should have inhalation valves with a low resistance to opening. One difficulty with low resistance valves is that aerosol leaks are more likely.[18]

Everard *et al.*[14] also showed that chamber agitation can reduce the dose delivered from a holding chamber and that a single large dose into a holding chamber is preferred over multiple actuations of small doses, which has been confirmed by Barry and O'Callaghan.[19]

Smaller VHCs may be viewed as less intimidating for infants and are easier for caregivers to handle.[14,20]

Around two decades ago, the publication of an *in vitro* benchtop study[21] showed that an antistatic lining can increase aerosol delivery from spacers by decreasing electrostatic VHC deposition rates. Numerous other studies since then have shown that limiting electrostatic effects can substantially increase drug output.[19,22-28] Despite this, the use of antistatic spacers in developing countries is still rare.

An early computed tomography (CT)-derived pediatric extrathoracic replica for benchtop study is the Sophia Anatomical Infant Nose-Throat (SAINT) model, which represents the nasal airway of a 9 month old Caucasian girl down to the subglottic level.[29] The female infant was scanned for an unrelated injury while under anesthesia and positioned on her back; the scan took around two minutes to complete.[29] The replica was made using a stereolithographical technique out of polymerized resin (Stereocol®).[29] This resin was found to interfere with high-performance liquid chromatography chromatograms and therefore upper airway deposition was not measured directly by chemical assay with this model.[29] However, the SAINT model can be cleaned with ethanol without significantly changing the internal geometry, as verified by repeated CT scans and resistance measurements.[29] Coatings to eliminate particle bounce and electrostatics in the SAINT model have been suggested but there is no consensus in the literature on an appropriate coating procedure, and concerns have been expressed about uneven coating distributions and coating reproducibility between runs.[30] Preliminary aerosol delivery measurements for different particle size fractions were performed

by Janssens *et al.*[29] using the experimental procedure shown in Figure 2, which is a modified form of the experimental setup developed by Finlay.[31]

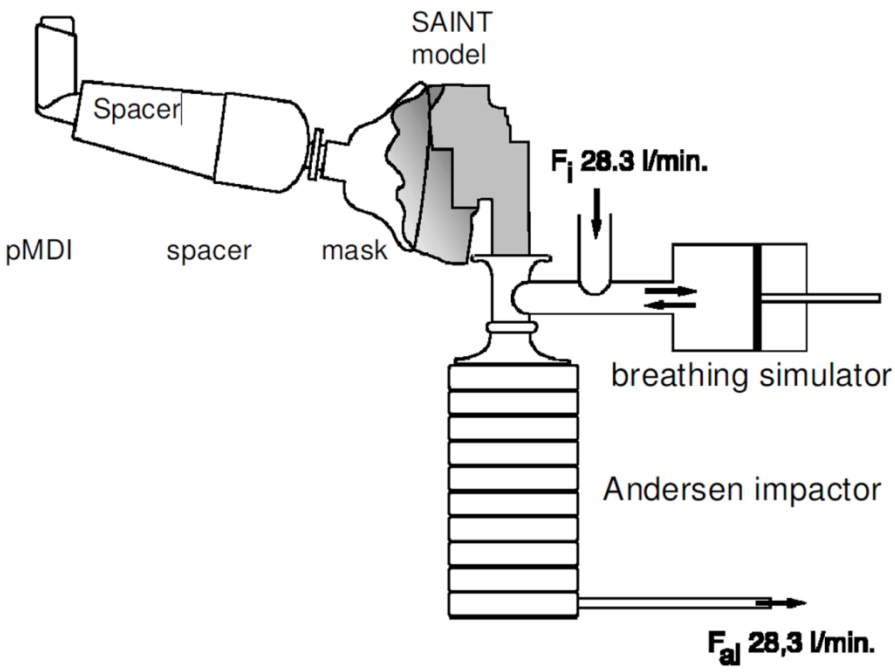

Figure 2: The experimental technique utilized by Janssens *et al*.[29] to determine the particle size distribution and dose delivered distal to the SAINT model via pMDI with VHC and face mask. Reprinted with permission from Ref. 29.

Using a similar benchtop study methodology, Janssens *et al*.[32] found that hydrofluoroalkane beclomethasone dipropionate (BDP) had a significantly higher proportion of extra fine particles (< 2.1 µm) passing through the SAINT model than chlorofluorocarbon BDP. The prospect of delivering pharmaceutical aerosol to toddlers by pMDI VHC face mask during sleep was also evaluated using the SAINT model;[33] however, an *in vivo* study found that 69% of children woke up during administration and they were often distressed.[34]

Another benchtop study with the SAINT model, utilizing the same setup shown in Figure 2, found that spacer output increases with tidal volume but is independent of respiratory rate while lung dose, which commonly refers to the dose reaching the trachea in benchtop studies, tends to decrease with increasing respiratory rate.[35] An initial increase and then decrease in lung dose was observed with increasing tidal volume.[35] Janssens *et al*.[35] also observed that upper airway deposition tended to increase with respiratory rate and tidal volume, fine particle dose tended to decrease with respiratory rate and tidal volume, while extra-fine particle dose was not affected by either.[35] Mass median aerodynamic diameter (MMAD) of the aerosol passing through the model decreased with increasing tidal volume or respiratory rate.[35] Putty was used to seal the face mask to the hard SAINT model face since a face mask leak can drastically reduce aerosol delivery.[5,35]

Esposito-Festen *et al*.[5] systematically quantified the relation between face mask leak size (in the range of 0 and 1.5 cm^2) and position of the face mask leak with spacer output and lung dose. A hole was drilled into round face masks, which were individually sealed to the hard SAINT model face using putty; the face masks were positioned with the hole location near the nose or near the chin.[5] Spacer output decreased for increasing leak size but was not related to leak position.[5] Lung dose decreased with increasing leak size, and decreased slightly more for leaks near the nose than for leaks near the chin.[5] Smaldone *et al*.[6] confirmed that face mask leakage significantly decreases the dose delivered for pMDI VHC face mask aerosol delivery, and observed that the decrease in dose delivered was greater than for face mask leakage with nebulizer-face mask aerosol delivery.

Producing a suitable aerosol is the first step of the pediatric aerosol delivery device development process, but designing a well-fitting face mask is crucial.[36-37] Therefore, studies using soft face models with the goal of better representing the face-face mask interface have recently become more common. Louca *et al*.[38] designed a soft face model utilizing silicone, where the face mask contacts the face, to measure orally inhaled particle mass for different VHC face mask combinations. Recent soft face models often use a soft, pliable silicone facial layer.[39-41] Recent experimental procedures have involved using cradles or shuttles to apply the VHC to a soft face model with a known force.[42-45] One such example used at Trudell Medical International is shown in Figure 3.

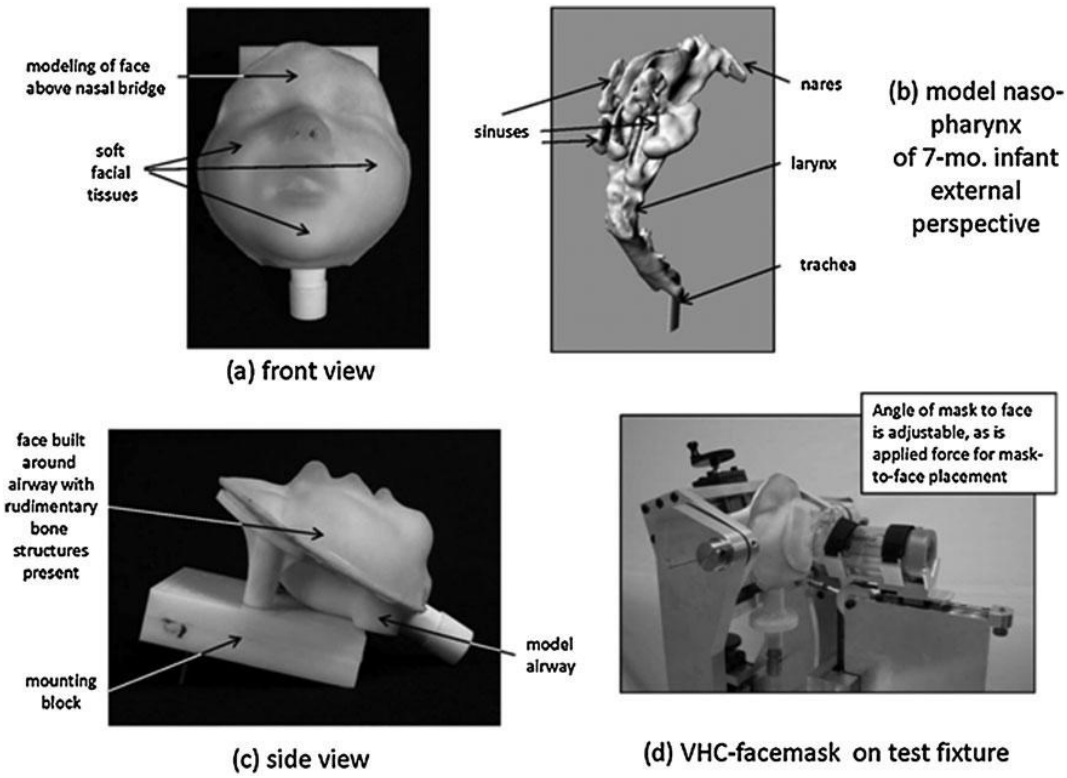

Figure 3: VHC face mask evaluation system used at Trudell Medical International.[45] Reprinted with permission from Ref. 45.

Studies with soft face models may be useful for comparing different VHC face masks. They can also be useful for determining the effect of face mask leakage on inhaled mass or lung dose in a clinically relevant manner *in vitro.*[45-46] However, a recent study found that N95 masks which fit well on adults *ex vivo* did not fit well on adult soft face models.[47] Therefore, even these soft facial materials may not be sufficient to mimic *ex vivo* face mask fit *in vitro*. However, a comparison of *ex vivo* - *in vitro* pharmaceutical aerosol face mask fit has not yet been published to the authors' knowledge.

1.3 Motivation and Objectives

'Fitted' mask dead volume and face mask seal may be affected by facial material softness and applied force. In this thesis, a quantitative comparison of mask dead volume, face mask seal, and lung dose for different applied 'push-on' forces and facial materials is presented. No study comparing mask dead volume, face mask seal, and lung dose for hard versus softer pediatric face models has been previously presented in the literature to the author's knowledge. This study determines if and when differences in inhaled pharmaceutical aerosol delivery exist between hard and soft face models, and is meant to be one step towards *in vitro* facial modeling. This study also represents a step towards the standardization of aerosol delivery device testing procedures with pediatric face and throat replicas.

1.4 Approach and Thesis Structure

Specifically, this study quantifies the dose of inhaled corticosteroid delivered distal to an idealized infant nasal airway geometry (taken as lung dose) for two clinically relevant applied forces, 1.5 lb and 3.5 lb[15] (6.7 N and 16 N; 0.68 kg and 1.6 kg), and using three different facial

materials. For the same applied forces and face mask-face contact locations as lung dose measurements, face mask seal is determined using flow rate measurements, while mask dead volume is determined using water displacement measurements. A mathematical model of lung dose based on face mask seal and mask dead volume is compared to experimental measurements.

Chapter 2 presents the materials and methods used in this study. First, the idealized infant geometry is discussed, followed by a description of the facial materials, throat materials, and aerosol delivery devices. Then, the methodology for verifying similarity in pressure drop between the throat and face replicas is described, as is the methodology for mask dead volume measurements, face mask seal measurements, and delivered dose measurements. The experimental technique for determining lung dose is described, as is a mathematical model for estimating lung dose based on mask dead volume and face mask seal. A description of the statistical analysis used in this study concludes Chapter 2.

Chapter 3 presents the verification of similarity in pressure drop between the throat and face replicas, as well as the mask dead volume, face mask seal, and lung dose experimental results. A comparison between the experimental measurements of lung dose and mathematical model predictions is also given.

Chapter 4 presents a discussion explaining the results, as well as comments on *in vitro* modeling and the applicability of this research to *in vivo* therapeutic aerosol delivery to infants.

Chapter 5 presents the conclusions to this study, including the study highlights, contributions to knowledge, and directions for future work.

CHAPTER 2: MATERIALS AND METHODS

2.1 Idealized Infant Geometry

The idealized infant geometry developed by Javaheri *et al*.[48] is shown in Figure 4.

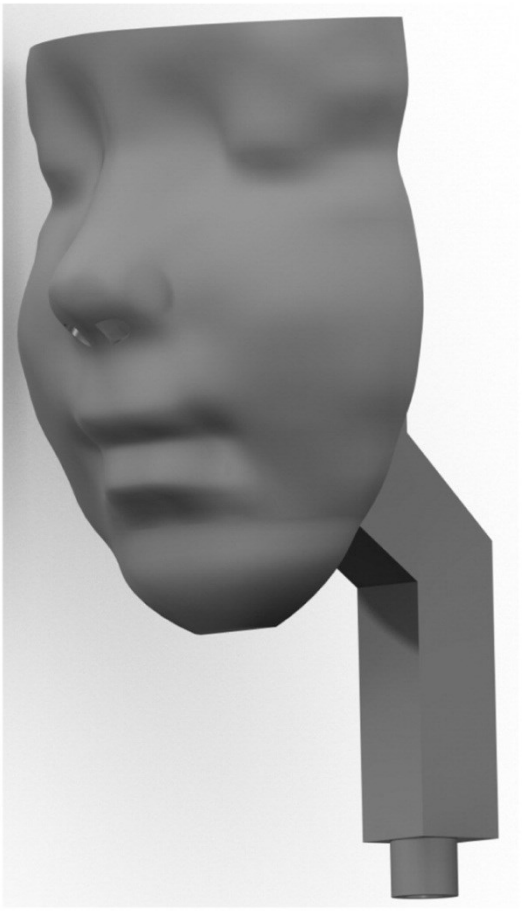

Figure 4: Idealized infant face and nasal airway geometry.[48] Reprinted with permission from Ref. 48.

This idealized geometry is a simplified analogue that incorporates average, pertinent dimensions measured in 10 of the CT-derived infant nasal airway replicas (3-18 months) presented by Storey-Bishoff *et al.*[49] and is designed to be representative of a one year old.

Relevant geometrical dimensions of the idealized infant nasal airway include an average hydraulic diameter of 4.8 mm, a minimum cross-sectional area perpendicular to expected airflow of 67 mm^2, an interior surface area of 9538 mm^2, and a nasal airway volume of 11.4 ml.[48]

2.2 Face Model Materials

A hard face model was replicated out of ABS (P430, Stratasys, Inc.; Eden Prarie, MN USA), a soft face model was replicated using a 5 mm layer of Shore 05A liquid silicone rubber (LSR-05, Factor II; Lakeside AZ, USA) on a polycarbonate (PC-ISO, Cimetrix Solutions Incorporated; Oshawa ON, CAN) facial backing, and a very soft face model was replicated using an 8 mm layer of Asker-C 0 polyurethane resin (Hitohada gel, EXSEAL Corporation; Mino City, Japan) on a polycarbonate facial backing. Figure 5 shows these three face models.

Figure 5: The three models used in this study. From left to right: ABS, silicone, and polyurethane.

The ABS face was replicated using an additive manufacturing machine (Dimension 1200es, Stratasys, Inc.; Eden Prarie, MN USA). The silicone face was replicated using a custom polycarbonate mold. The polyurethane face was replicated using a hard polycarbonate mold shell with a softer interior mold made from Tango Plus (Stratasys Incorporated; Eden Prairie MN, USA) to help with mold release. The polycarbonate face backings had simplified facial counters, roughly representing bone structure, and were created using a 3D printer (Fortus 400mc, Cimetrix Solutions Incorporated; Oshawa ON, CAN). The silicone and polyurethane

facial layers were sealed to their respective polycarbonate backings at the outer edges using cured GE Silicone I (GE Sealants and Adhesives; Huntersville NC, USA). The outer surfaces of the ABS face and polycarbonate facial backings were dissolved in dichloromethane (Sigma-Aldrich; St. Louis MO, USA) to eliminate air permeability. The surface coating agent available from the polyurethane manufacturer to decrease the polyurethanes stickiness was not used since it was deemed a hazardous material and could not be imported to Canada from Japan.

The ABS face is essentially non-deformable. The Shore 05A silicone facial layer deforms slightly (a few tenths of a mm) to the light push of a finger. The Shore 0A polyurethane resin is claimed by the manufacturer to be as soft as baby's skin[50] and was hence hypothesized to be the most realistic. It deforms a few mm to the light push of a finger. As a further indicator of facial material softness, one may refer to the mask dead volume results in Section 3.2.

2.3 Throat Materials

All faces use the same detachable resin throat replicated out of VeroClear (RGD810, Stratasys Incorporated; Eden Prairie MN, USA) resin on an Objet Connex 3D Printer (Stratasys Incorporated; Eden Prairie MN, USA). The VeroClear throat has a detachable VeroWhite (FC830, Stratasys Incorporated; Eden Prairie MN, USA) septum also replicated on the Objet Connex 3D Printer. The outer surface of the VeroWhite septum was dissolved in dichloromethane to eliminate air permeability. The throat is shown in Figure 6.

Figure 6: VeroClear throat with detachable VeroWhite septum.

2.4 Aerosol Delivery Devices

A Qvar® (Medicis Pharmaceutical Corporation; Scottsdale AZ, USA) pMDI with a 100 µg nominal dose was used. An AeroChamber Plus Flow-Vu™® VHC with Small Mask (Trudell Medical International; London ON, CAN) was chosen. The volume of the antistatic VHC is 149 ml.[51] The mask is made of flexible silicone and has a 40 ml static mask dead volume.

2.5 Airway Pressure Drop Methods

To verify a similar pressure drop between the face models, a rotary vane (positive displacement) vacuum pump (Model 0523-101Q-SG588DX, Gast Manufacturing, Inc.; Benton Harbor, MI USA) was used to displace air through a valve, flow meter (TSI Model 4043; Shoreview, MN USA), and tubing at a flow rate of 6 l min^{-1} for each face model with the same

throat. The pressure drop through the replica was estimated by subtracting the absolute pressure reading for flow with the replica connected to the tubing, to flow through only the tubing. Pressure and flow rate were recorded at a 1 Hz frequency. The recorded pressure readings had a 10 Pa resolution. Averages of flow over 5 seconds without the replica and over 10 seconds with the replica were used for calculation.

The putty seal required between each face model and the throat, as well as the seal between the silicone and polyurethane facial layers and their polycarbonate facial backings, was also verified using the same flow setup by closing the nostrils and observing a substantial decrease in absolute throat pressure (vacuum formation) at 45 l min^{-1}.

2.6 Mask Dead Volume Methods

A force measurement system consisting of a TOL-09141 Digital Multimeter (SparkFun Electronics; Boulder CO, USA), in-house amplifier, and FUTEK LTH300 Donut Load Cell (FUTEK Advanced Sensor Technology, Inc.; Irvine CA, USA) was calibrated by placing calibration weights (80850138 and 80850130, Ohaus Corporation; Pine Brook NJ, USA) on the load cell and reading the voltage output from the multimeter. From this calibration the voltage output per pound of applied force was determined.

The frontpiece was removed from a VHC and the face mask was given a water-tight seal at the outer (ambient) side of the exhalation valve and at the inner (face mask) side of the inhalation valve using cured silicone rubber. By sealing the inner side of the inhalation valve the Flow-Vu™® indicator valve path was also blocked. The nostrils of the faces were sealed to ensure no water displacement into them.

Figure 7 shows a schematic of the mask dead volume measurement system which is a modified form of that presented by Shah *et al.*[15] A petri dish was placed on the load cell. The face mask was completely filled with 40±0.5 ml of water. The face mask did not noticeably deform due to the weight of the water. The weight of the petri dish, VHC frontpiece, and 40 ml of water filling the face mask was determined and an additional 1.5 lb and 3.5 lb of force corresponded to the total force applied to the load cell during mask dead volume measurement.

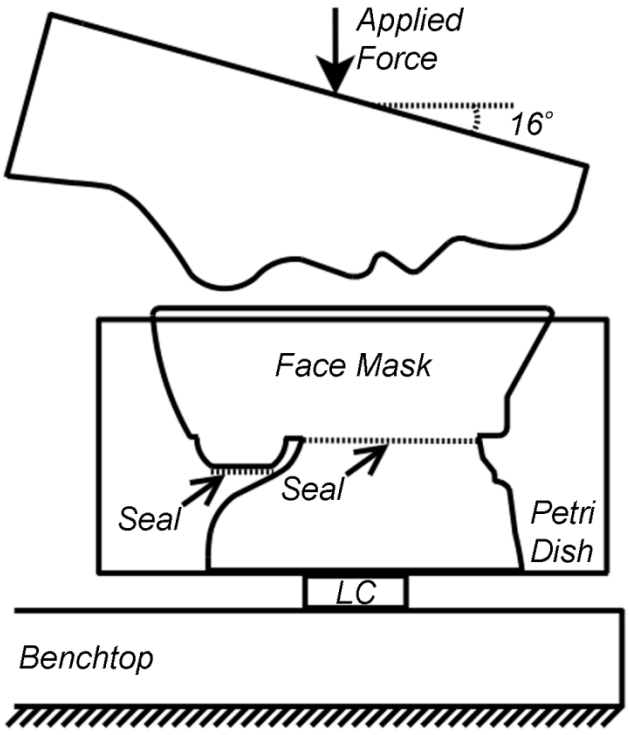

Figure 7: Schematic of the mask dead volume measurement system. LC: load cell.

The face was lined up with the face mask and tilted 16° to ensure the best fit. Lines were drawn at an angle of 16° on a wooden board, which was placed behind the measurement system to assist with angle tilt adjustment. The face was slowly lowered onto the face mask

with increasing force until 1.5 lb or 3.5 lb was applied. This caused water displacement from the face mask into the petri dish. The petri dish captured the displaced water, to ensure any loss of water mass from the face mask did not affect the applied force measurement. After the desired applied force was achieved the face was removed from the face mask. Water absorption onto the faces was negligible and it was verified that no water was displaced into the nasal airways. The water remaining in the face mask was poured into a graduated cylinder, from which the mask dead volume under the condition of an intruded face with a known applied force to the face mask was read.

Any free surface of water within the face mask when the face is applied represents a pathway for leakage to occur. It is necessary that this free surface exists in order for water displacement to occur. Therefore, the presence of continual water displacement indicates the absence of a complete face mask seal. In the case of the polyurethane face a complete face mask seal prevented continual water displacement from the face mask as the applied force was increased. This complete face mask seal may have been due in part to the stickiness of the polyurethane material or softening with water. An estimate of the mask dead volume for the polyurethane face was needed, and therefore the polyurethane face was applied to the face mask with the left cheek higher than the right cheek with an angle relative to the horizontal of approximately 25° to allow for water displacement. The ABS and silicone faces did not form a complete seal for any tested applied force and were therefore applied symmetrically. Analysis was performed using the results of three trials for each test.

2.7 Face Mask Seal Methods

A schematic of the face mask seal measurement system built in-house is shown in Figure 8. The VHC was placed in a vertical wood plate which contains a 1.75" [44.45 mm] circular hole. The position of a vertical wood plate was adjusted and fixed using nuts and bolts to set the desired applied force. The vertical wood plate makes contact with two load cells which send output signals through two separate in-house amplifiers to multimeters, from which the voltage output was read. Each load cell transfers half of the applied force to a flat acrylic plate containing a 1.75" [44.45 mm] circular hole for the VHC. An annular hard plastic press fitting with an inner diameter of 44 mm, outer diameter of 60 mm, and length of 15 mm transfers the applied force from the acrylic plate to the VHC. The annular press fitting was designed in SolidWorks and built in-house at the machine shop. Due to the slight taper of the VHC the press fitting could be easily and repeatedly removed and refitted. The throat was inserted through a hole in the hinge plate. A stationary wood plate was connected by a hinge to the hinge plate and screwed to the bottom wood plate (and reinforced with metal) to ensure it remained fixed. C-clamps held the bottom plate to the bench top. Flex of the hinge plate is prevented by contact at three locations, forming a triangle, with fully threaded bolts held in place using female fittings in the stationary wood plate. The angle of the hinge plate was adjusted to approximately 16° for all tests by turning these threaded bolts. Face mask seal was measured by drawing air through the throat at the experimentally determined average inhalation flow rate during tidal breathing for lung dose measurements of 4.26 l min^{-1} (as measured by a flow meter), and by comparing to the flow rate through the VHC, Q_{VHC} was measured using a flow meter (here only TSI Model 4143; Shoreview, MN USA) connected to the VHC via tubing

inserted just through the boot. Analysis was performed using the results of three trials for each test.

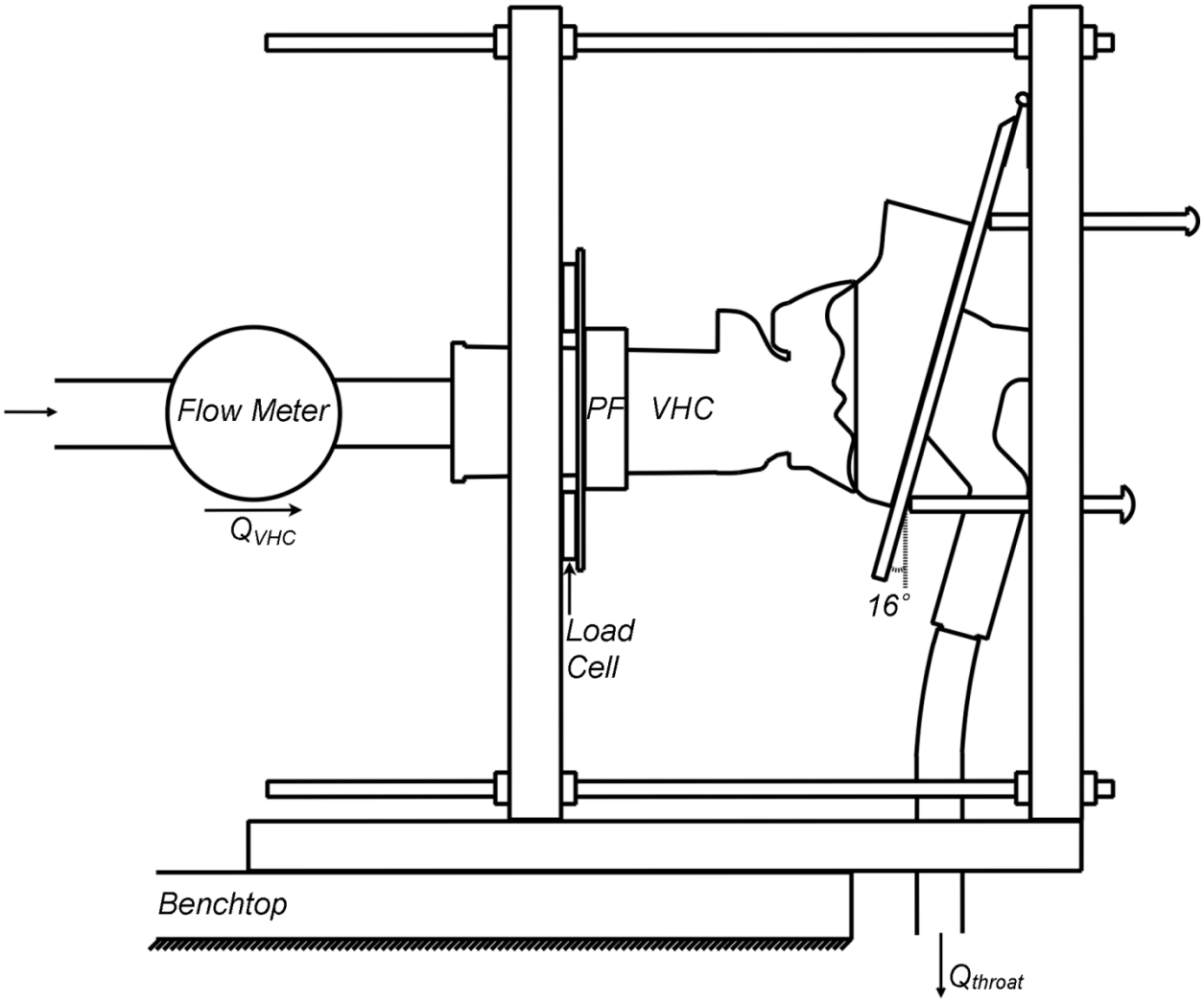

Figure 8: Schematic of face mask seal measurement system. Q_{VHC}: air flow rate through the VHC for Q_{throat}=4.26 l min^{-1} of air flow rate through the throat; PF: 44 mm inner diameter press fitting on the slightly tapered VHC.

2.8 Delivered Dose Methods

Delivered (ex-actuator) dose was measured by spraying the pMDI directly to a filter (Respirgard II™ 303, Vital Signs Incorporated; Englewood CO, USA). A custom press-fitting designed using SolidWorks and built in-house connected the pMDI to the filter.

The efficiency of these low pressure drop filters is quoted[52] as 99.9% for bacterial filtration efficiency and 99.8% for viral filtration efficiency, which were determined using 2.7-3.3 µm particles; however, the MMAD of Qvar® is 1.1 µm. Hence, filter efficiency testing was performed. Since particle capture efficiency may increase with flow rate due to increased particle impaction on the filter fibers, delivered dose was measured at 15 l min^{-1} increments from 15 l min^{-1} to 60 l min^{-1} (passing through the filter), as initiated by a vacuum pump, set by a valve, and read by a flow meter. Three trials were performed at each flow rate.

BDP deposition on the filter was analyzed using ultraviolet-visible (UV) spectrophotometry (8452A Diode Array Spectrophotometer, Hewlett-Packard; Mississauga ON, CAN) at a wavelength of 238 nm.

2.9 Experimental Lung Dose Methods

Initially, lung dose experiments were performed by slightly modifying the setup shown in Figure 8. A filter was placed at the distal end of the throat and a pMDI was inserted in the VHC boot. The distal end of the filter was connected to tubing leading to a breathing simulator. Initial experiments showed that a highly variably and usually low BDP dose was recovered. After parametric error testing and delivered dose measurements, it was found that the filters were not efficient at capturing the small BDP particles at the low flow rates associated with an infant

respiratory cycle. In addition, filter housing dead volume undesirably decreased the volume of aerosol reaching the filter fibers in a given breath. Therefore, a bias flow system was developed to supply a sufficiently high, constant flow rate through the filter during lung dose measurements to ensure adequate filter efficiency, while also eliminating the filter housing dead volume issue.

Figure 9 shows a schematic of the bias flow system used to measure lung dose. Figure 10 shows a picture of the lung dose measurement system. A custom tee connects the throat to upstream flow from a compressed air supply and an in-house positive displacement breathing machine (known in the laboratory as the Happy Breathing Machine) and to downstream flow to a vacuum pump. The distal end of the throat was inserted directly into the tee. A bias air supply flow rate of 45 l min^{-1} from a compressed building supply line was set using a valve and measured with a flow meter. This flow was balanced by a 45 l min^{-1} flow rate to a vacuum pump as set by a valve and measured with a flow meter. The breathing machine initiates the desired breathing pattern through the throat, while a constant bias flow rate of 45 l min^{-1} passes through the filter. The bias flow rate is considerably higher than the flow rate through the throat and so minimal deposition by impaction was expected on the tee. This system eliminates the effect of the 20 ml filter housing dead volume on the lung dose since in this setup all flow passing immediately distal to the throat reaches the filter fibers. It was verified that during balanced bias flow without breathing simulation the Flow-Vu™® indicator valve did not move, indicating no flow through the VHC.

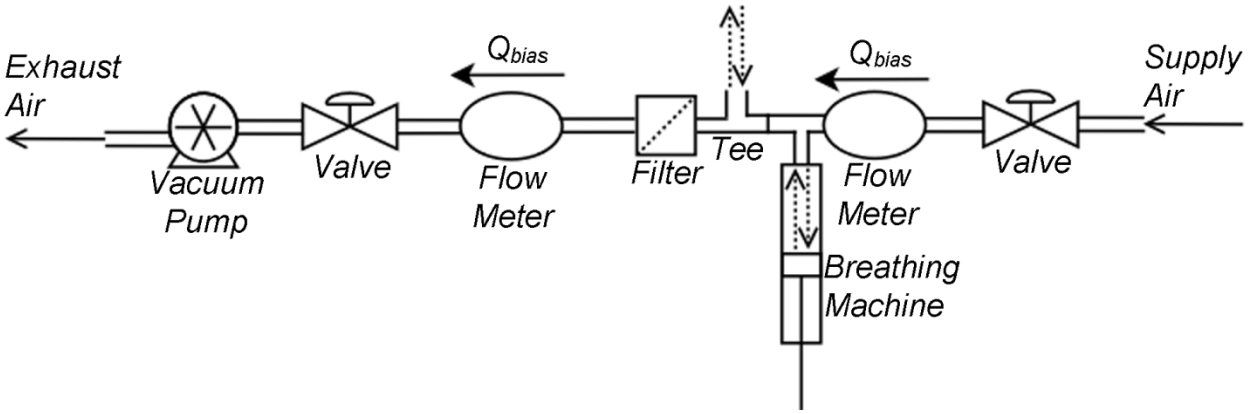

Figure 9: Schematic of the bias flow system used to measure lung dose. The throat was inserted into the top of the tee and positioned in the setup previously shown in Figure 8, with the flow tubing in the VHC boot in Figure 8 replaced by the pMDI. Supply air was from a compressed building supply line. This system utilizes a bias flow rate of Q_{bias}=45 l min^{-1} to eliminate filter inefficiency and dead volume issues.

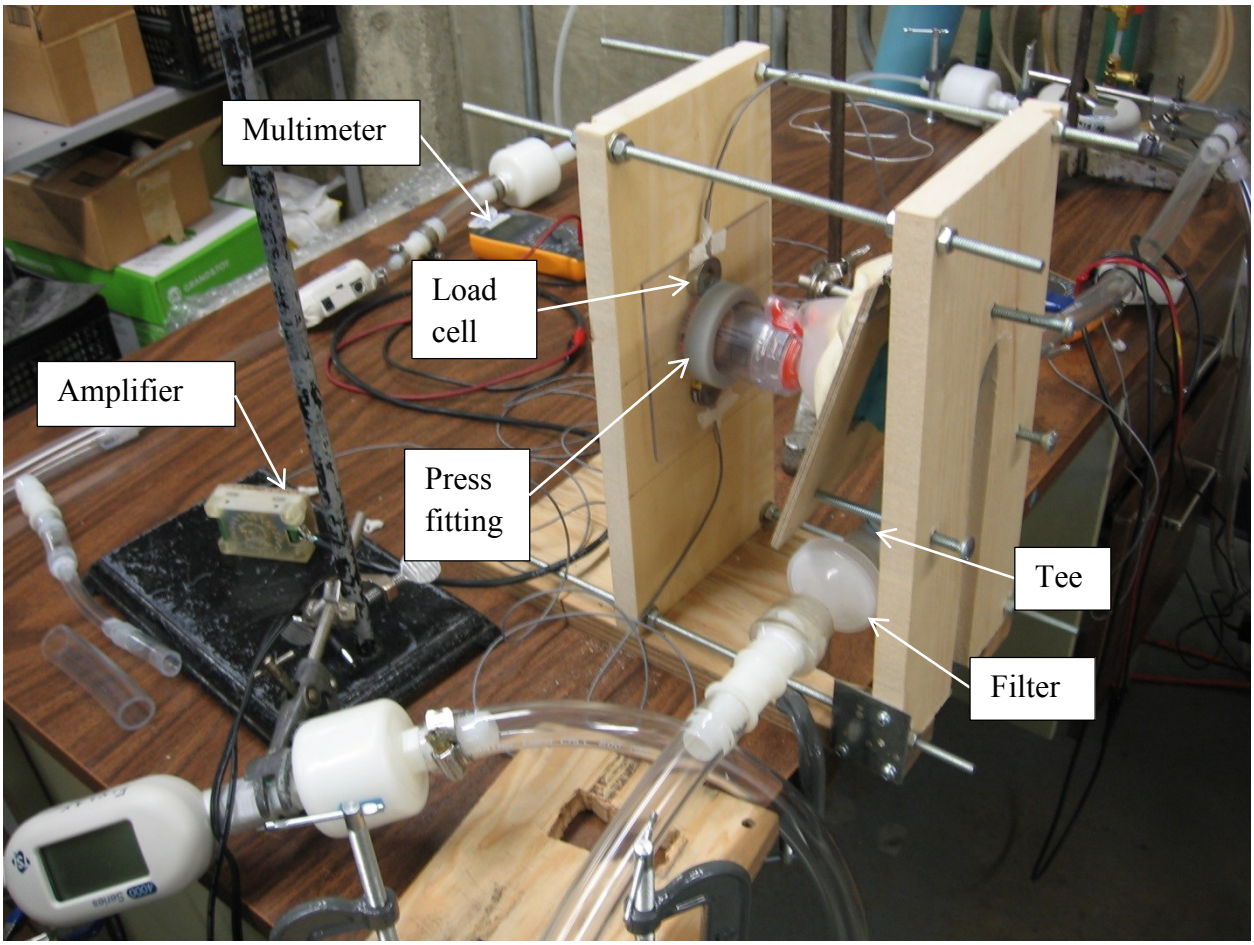

Figure 10: Picture of the lung dose measurement system. The position of the wooden plate on the left was adjusted and fixed using nuts and bolts to apply a constant measured force from the VHC to the face.

The breathing machine was programmed to create a 50 ml inhalation breath lasting 0.5 seconds followed immediately by a 50 ml exhalation breath lasting 1.5 seconds, as per the Canadian Standard CAN/CSA/Z264.1-02: Spacers and holding chambers for use with metered-dose inhalers.[53] Simple sinusoids were programmed for the inhalation and exhalation curves. This required iteratively changing the programmed breathing machine input as the average breathing frequency, as measured over many respiratory cycles using a stopwatch, was higher

than the programmed frequency. However, even after these breathing pattern corrections, due to flow interactions in the lung dose measurement system, the flow pattern through the throat differed from the breathing machine output. The flow pattern through the throat was estimated by replacing the throat with tubing leading to a flow meter. The resulting flow pattern is shown in Figure 11. The measured flow pattern had a 0.65 second inhalation time with a 46.1 ml inhalation volume, followed by a 1.43 second exhalation with a 49.6 ml exhalation volume. The average inhalation flow rate was 4.26 l min^{-1} and the average exhalation flow rate was 2.09 l min^{-1}. Peak inspiratory flow rate was 6.55 l min^{-1} and peak expiratory flow rate was 2.60 l min^{-1}.

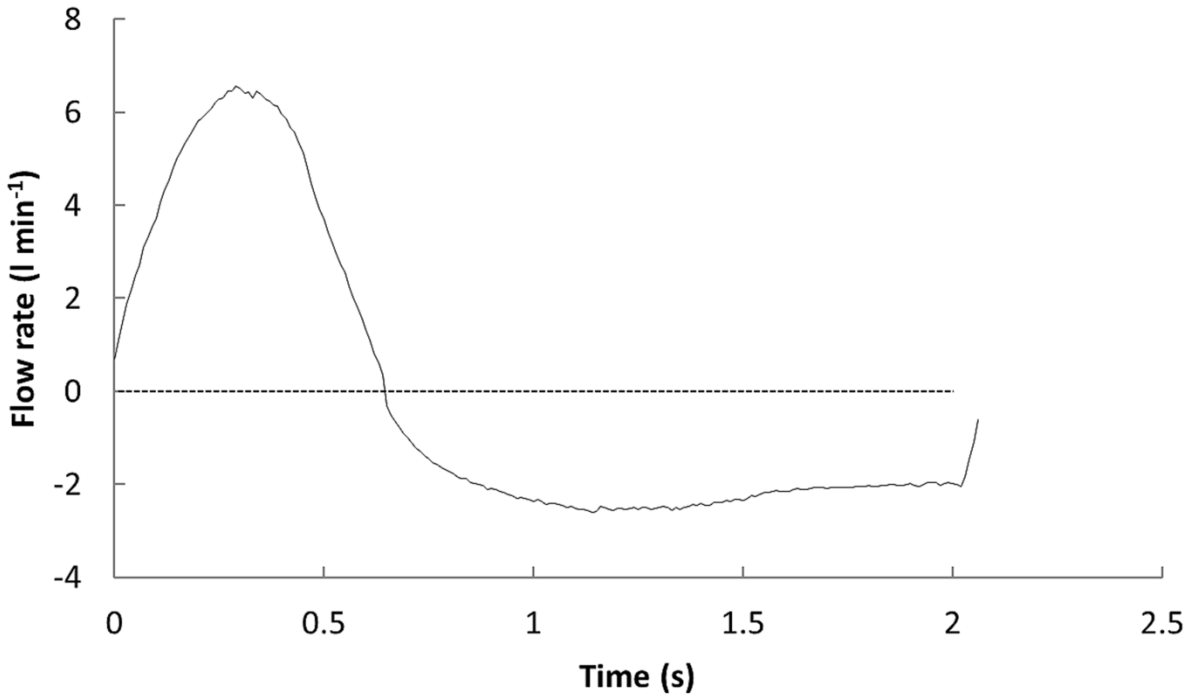

Figure 11: Measured flow rate representing a single breathing cycle within the throat. Sampling frequency was 100 Hz. Flow meter response time is 4 ms and accuracy is 0.05 slpm or 2% of reading, whichever is less.

Lung dose measurements were performed by actuating the pMDI at the onset of inhalation as per the Canadian Standard[53] recommendation for simulating perfectly coordinated aerosol delivery. A total of 6 breaths were simulated after actuation occurred as per pamphlet instructions and then breathing simulation was terminated. Only one actuation was performed per test. The vacuum pump was shut off prior to closing the supply air valve in order to prevent additional inhalation through the VHC. The filter was removed and later analyzed by UV spectrophotometry. Analysis was performed using the results of three trials for each test, with the exception of ABS at 3.5 lb, for which the results of only two trials were analyzed.

The temperature and relative humidity were measured using an HM70 Vaisala HUMICAP® Hand-Held Humidity and Temperature Meter (MI70 Measurement Indicator, HMP75B Humidity and Temperature Probe, Vaisala Oyj; Helsinki, Finland). All lung dose measurements took place over two days, during which the temperature and relative humidity were 21˚C and 45%RH on the first day and 22˚C and 30%RH on the second day. Measurements with polyurethane were performed on the first day, with silicone on both days, and with ABS on the second day.

Previously, Laube *et al*.[30] expressed concerns about eliminating particle bounce and electrostatic effects using airway surface coatings, due to the possibility of an uneven airway surface coating distribution and reproducibility between runs. Therefore, to minimize experimental discrepancy between runs, no coating was used for the airway surfaces. To verify that electrostatic effects were negligible and particle bounce was not an important factor, on

the second day after all lung dose measurements, a run at 3.5 lb was performed after coating the custom tee, the silicone face, and the nasal airways of the silicone face and VeroClear throat with a 0.5% benzalkonium chloride (Sigma-Aldrich; St. Louis MO, USA) solution in alcohol (Reagent A.C.S., Fisher Scientific; Mississauga ON, CAN). This coating is electrically conductive, is used in cationic detergents, and is hygroscopic, creating a water film on the surface which can lessen particle bounce. It was verified that with this coating the lung dose was within the range of that measured without a coating, indicating the coating had a negligible effect on the measured lung dose. Only a single VHC was used in this study since variability in lung dose using different VHCs from the same supplier was substantial. Rinsing the VHC was found to render the inhalation valve useless. The difference in electrostatics within the single VHC used in this study after multiple actuations was assumed to be negligible since similar lung dose measurements were found between successive runs. After all lung dose measurements were completed, breathing simulation was performed in the same manner as during lung dose measurement, but without actuation of the pMDI. It was thus found that 0.7 µg of particle re-entrainment from the pMDI, VHC, face mask, airways, and (or) tee reached the filter, which was deemed acceptably small compared to the lung dose, with the sole exception of ABS at 1.5 lb.

2.10 Mathematical Lung Dose Model

During a single breath, the volume of aerosol reaching the lungs (V_a) is given by:

$$V_a = V_t - V_L - a * MDV - b * V_{NA} \quad (1)$$

where V_t is the tidal volume equal to 46.1 ml for inhalation, V_L is the volume of air inhaled from face mask leaks, MDV is the measured mask dead volume, and V_{NA} is the nasal airway volume

equal to 11.4 ml for the idealized infant replica.[48] The correction factor a represents the fraction of the MDV air inhaled prior to the inhalation of aerosol, and is approximated as 0.1 for this study due to expected aerosol streaming. The correction factor b represents the fraction of the air in the nasal airway inhaled prior to the inhalation of aerosol, and is approximated as 0.9 for this study. The correction factors a and b could be more accurately estimated using computational fluid dynamics results, but this was outside the scope of this study. The difference between the tidal volume and the volume of air inhaled from leaks, $V_t - V_L$, is equal to the volume of aerosol exiting the VHC in a single breath. This difference is known from face mask seal measurements and is given by:

$$V_t - V_L = Q_{VHC} * t_i \tag{2}$$

where Q_{VHC} was defined in Section 2.7 and the inspiration time t_i is 0.65 seconds. Equation (2) assumes that the inhalation valve opens immediately at the start of inhalation.

The lung dose for the first breath (LD_1) is the volume of aerosol reaching the lungs multiplied by the aerosol concentration (C_a) and the fraction of aerosol not deposited to the nasal airways:

$$LD_1 = V_a * C_a * (1 - \eta) \tag{3}$$

where η is the extrathoracic deposition fraction approximated as a constant value of 0.024 in this study based on Javaheri *et al*.[48] and a 1.1 µm MMAD. The aerosol concentration is assumed to be constant for a given breath and for the first breath is given by:

$$C_a = \frac{ED * DD}{V_{VHC}} \quad (4)$$

where ED is the fraction of the delivered ex-actuator dose, DD, initially available for inhalation from the VHC (approximated as 0.27 based on direct measurement in a study with an AeroChamber and Budesonide[54] and the maximum lung dose for a study with an AeroChamber and BDP[32]). The VHC volume V_{VHC}=149 ml[51].

The mass of aerosol in the VHC decreases for each breath and hence the aerosol concentration in the VHC decreases. The fraction of aerosol remaining in the VHC after a single breath (RF) is given by:[55]

$$RF = \left[1 - \frac{V_t - V_L}{V_{VHC}}\right] e^{\frac{\ln(1/2)}{T_{1/2} f}} \quad (5)$$

where the exponential term represents the fraction of aerosol in the VHC not lost to sedimentation after one respiratory cycle, with $T_{1/2}$ equaling the aerosol half-life taken as 30 seconds for the present antistatic VHC and f equaling the respiratory cycle breathing frequency of 0.48 Hz. The results are very insensitive to the choice of $T_{1/2}$.

Zak *et al.*[55] related the fraction of aerosol inhaled in a single breath and the remaining fraction of aerosol in a VHC to the accumulated fraction of aerosol inhaled in *n* respiratory cycles. Here, the analysis is slightly modified to relate the lung dose for a single breath, LD_1, and the remaining fraction of aerosol in the VHC, RF, to the accumulated lung dose in *n* respiratory cycles (LD).

The lung dose for the i^{th} breath (LD_i), in a series of *n* respiratory cycles, is:

Respiratory cycle, *i*	$\boldsymbol{LD_i}$
1	LD_1
2	$LD_1 * RF$
3	$LD_1 * RF^2$
.	.
.	.
.	.
n	$LD_1 * RF^{n-1}$

Equivalently, $LD_i = LD_1 * RF^{i-1}$. This assumes that no aerosol re-enters the VHC after exiting, i.e. perfect inhalation valve function, and that the face mask and nasal airways are cleared of aerosol by expiration. Here, RF^{i-1} accounts for the decrease in aerosol concentration for each breath. In this study, the total number of respiratory cycles n = 6.

To obtain the total lung dose, LD, the lung dose for each respiratory cycle, LDF_i, are summed over all respiratory cycles ($i = 1 \rightarrow n$):

$$LD = LD_1 * (1 + RF + RF^2 + \cdots + RF^n) \quad (6)$$

Using a geometric series, this equation can be rewritten:

$$LD = LD_1 * \frac{1 - RF^n}{1 - RF} \quad (7)$$

LD predictions were constrained to be greater than or equal to zero. A sample calculation using the mathematical lung dose model for ABS at 3.5 lb is given in Appendix A.

2.11 Statistical Analysis

A two-sided 95% confidence interval (CI), which assumes a normal distribution, was calculated for all tests and significance statements are based on a lack of CI overlap.

CHAPTER 3: RESULTS

3.1 Airway Pressure Drop Results

Time-averaged airway pressure drop for all faces with the throat were within the 40-50 Pa range, indicating that variations in pressure drop due to differences in airway materials and uncompressed geometry of the face models were negligible, as expected.

3.2 Mask Dead Volume Results

Table 1 gives the mask dead volume after application of each face model at 1.5 lb and 3.5 lb of force. Mask dead volume was slightly less than half of the inhalation tidal volume (46.1 ml) for the ABS face at 1.5 lb of force, and on average slightly more than one-quarter of the tidal volume for the very soft polyurethane face model at 3.5 lb of force.

Table 1: Mask dead volume (MDV), in ml, for ABS, silicone, and polyurethane face models applied at 1.5 lb and 3.5 lb of force. Results reported as mean (95% CI).

Force (lb)	MDV - ABS	MDV - Silicone	MDV - Polyurethane
1.5	22.5 (21.9-23.1)	21.2 (20.3-22.0)	19.7 (19.0-20.3)
3.5	14.8 (14.5-15.2)	14.3 (13.7-15.0)	12.5 (11.9-13.1)

3.3 Face Mask Seal Results

Table 2 gives the flow rate through the VHC, Q_{VHC}, for each face model at 1.5 lb and 3.5 lb of force. Almost no air was inhaled from the VHC when the hard ABS face was used at 1.5 lb indicating a great deal of face mask leakage. Similarly, low values of Q_{VHC} were found for the

silicone face at 1.5 lb. At 3.5 lb, just more than half of the flow through the throat came from the VHC with the ABS face, and nearly three quarters came from the VHC with the silicone face. The seal obtained with the polyurethane face at 1.5 lb was better the seal obtained with either the ABS or silicone face at 3.5 lb. All differences in Q_{VHC} between face models at the same applied force were significant. The polyurethane face was found to form a complete seal with the face mask at 1.5 lb and 3.5 lb during mask dead volume measurements. Q_{VHC} was not found to be 4.26 l min^{-1} for polyurethane which was likely due to leaks within the VHC system.

Table 2: Q_{VHC}, in l min^{-1}, for ABS, silicone, and polyurethane face models applied at 1.5 lb and 3.5 lb of force. Results reported as mean (95% CI).

Force (lb)	Q_{VHC} - ABS	Q_{VHC} - Silicone	Q_{VHC} - Polyurethane
1.5	0.03 (0.00-0.06)	0.23 (0.17-0.29)	3.60 (3.48-3.72)
3.5	2.32 (2.27-2.37)	3.10 (3.08-3.11)	3.76 (3.73-3.79)

3.4 Delivered Dose Results

Figure 12 shows delivered dose for the different tested flow rates. Measured delivered dose of BDP was not significantly different between any tested flow rate greater than or equal to 30 l min^{-1}. However, delivered dose was most consistent at 45 l min^{-1}, which was chosen as the bias flow rate for lung dose measurements. Mean (95% CI) delivered dose at 45 l min^{-1} was 80.4 (76.9-83.9) µg. Without bias flow, the use of multiple filters in series was found to significantly lower the total captured dose relative to the use of only one filter, possibly for electrostatic

reasons. In addition, the second filter repeatedly captured 20-32% of the dose captured by the first filter when placed in series.

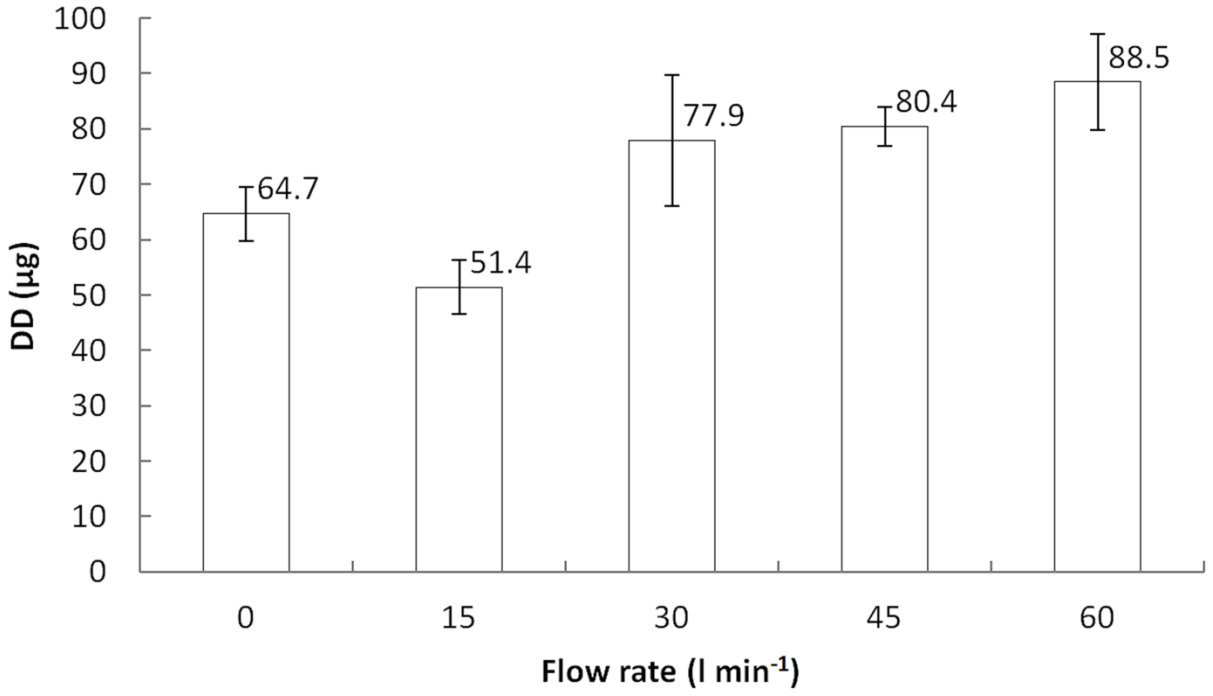

Figure 12: Measured delivered dose (DD) for different flow rates through the filter during pMDI actuation.

3.5 Experimental Lung Dose Results

BDP lung dose for each facial material and applied force is given in Table 3. The use of softer facial materials increased the measured lung dose at 1.5 lb. For example, at this force the difference in mean lung dose between polyurethane and silicone was 16.9 µg, and was statistically significant. On the other hand, at 3.5 lb the difference in mean lung dose between polyurethane and silicone was 0.4 µg and was not statistically significant.

Table 3: Lung dose (LD), in µg of BDP, delivered through an idealized infant nasal airway by a 100 µg Qvar® pMDI via an AeroChamber Plus Flow-Vu™® VHC with Small Mask applied at 1.5 lb and 3.5 lb of force to ABS, silicone, and polyurethane face models. Results reported as mean (95% CI).

Force (lb)	LD - ABS	LD - Silicone	LD - Polyurethane
1.5	0.9 (0.3-1.6)	2.4 (0.2-4.6)	19.3 (18.3-20.3)
3.5	10.0 (7.9-12.0)	13.8 (12.2-15.4)	14.2 (13.2-15.2)

For the ABS face model and the silicone face model, lung dose was greater at 3.5 lb than at 1.5 lb. For the polyurethane face model, lung dose was less at 3.5 lb than at 1.5 lb. This is likely since the extreme softness of the polyurethane facial layer resulted in the nose nearly touching the exhalation valve and the mouth nearly touching the inhalation valve casing at 3.5 lb, which may have increased facial deposition or distorted the face mask enough to affect valve function.[16]

The lung dose reported here is slightly lower than the mean value of 25.4% given by Janssens *et al*.[32] for a similar tidal volume using the SAINT model with a perfect face mask seal and an unknown applied force. This is likely due to differences in the experimental procedure including the use of a different extrathoracic geometry, as well as the use of 1 puff and filters in this study rather than 10 puffs and an impactor in the study by Janssens *et al*.[32].

The speed of the Flow-Vu™® indicator valve motion during lung dose measurements appeared to relate well with face mask seal.

3.6 Mathematical Lung Dose Model Results

Figure 13 presents the experimental lung dose measurements next to the mathematical predictions based on experimentally measured mask dead volume and face mask seal. The mathematical model predicts lower lung dose than experimental measurements. This is expected since the model assumes the face mask and the nasal airways are completely cleared of aerosol during exhalation. At 3.5 lb, experimental measurements and mathematical predictions of lung dose are closer, most likely because the mathematical model does not account for facial deposition. As an indicator of the expected facial deposition, Erzinger *et al*.[4] found 2.6-7.9 µg of facial deposition on young children *in vivo* after treatment with salbutamol via 100 µg pMDI with AeroChamber VHC and face mask.

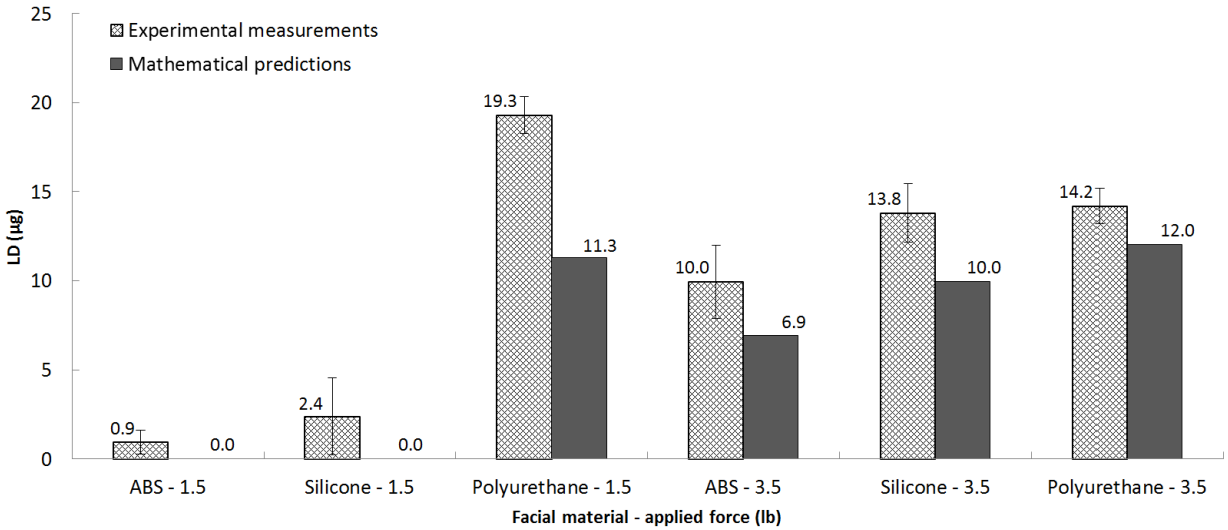

Figure 13: A comparison of experimental lung dose (LD) measurements and mathematical LD predictions. Values of MDV for use in equation (1) were taken from Table 1, values of Q_{VHC} for

use in equation (2) were taken from Table 2, values of LD for the mathematical predictions are based on equation (7), and experimental measurements of LD were taken from Table 3. Error bars encompass 95% CI.

A parametric analysis with the mathematical model showed that at the same applied force, differences in mask dead volume between face models had little impact on the predicted lung dose (0.1 μg or less). On the other hand, differences in mask dead volume for the same face model between applied forces had a larger impact on the predicted lung dose (0.4 μg or less). When Q_{VHC} was matched for all face models at the same applied force, similar lung dose predictions were found for the face models (differing at most by 0.1 μg). In addition, when Q_{VHC} for each face model at 1.5 lb was changed to that measured for the same face model at 3.5 lb, lung dose predictions at 1.5 lb were similar to those at 3.5 lb (and vice versa, differing at most by 0.4 μg). Hence, Q_{VHC} from experimental measurements was essentially predictive of lung dose according to the mathematical model. This indicates that the differences in face mask seal between face models had a larger impact on lung dose than the differences in mask dead volume. These conclusions are the same when the MDV and nasal airway dead volume correction factors are changed to a=1 and b=1, respectively.

CHAPTER 4: DISCUSSION

4.1 Evaluation of Results

Three lung dose regimes were observed: 1) minimal lung dose for ABS and silicone at 1.5 lb; 2) intermediate lung dose for all three face models at 3.5 lb; and 3) maximal lung dose for polyurethane at 1.5 lb. The minimal dose for ABS and silicone at 1.5 lb was due to the lack of a tight face mask seal. This lung dose is expected to be even lower with a similarly shaped rigid face mask material as compared to the present flexible silicone face mask material. Lung dose was less for all three face models at 3.5 lb than for polyurethane at 1.5 lb, possibly due to greater facial and face mask deposition at 3.5 lb, particularly for polyurethane.

4.2 Comments on *In Vitro* Modeling

When comparing different pMDIs with the same VHC, it is often necessary to form a sufficiently tight face mask seal to ensure lung dose consistency. Even leaks which were visually very small led to drastic decreases in flow rate through the VHC. Two reasonable options for obtaining a tight face mask seal *in vitro* are: a) using a sealant with a hard face model; and b) using a sufficiently soft face model.

At the same applied force, face mask seal was predicted mathematically to be a greater factor in determining the difference in lung dose between face models than mask dead volume. Therefore, at the same applied force the use of a sealant such as glue or putty with a hard face may be a reasonable alternative to a very soft face model, as in either case a complete seal can be obtained with negligible differences in mask dead volume. However, the sealant should be applied while the applied force is being maintained, as the face mask tends to flex outwards on

the face with increasing applied force and the mask dead volume can decrease significantly with increasing applied force relative to the tidal volume. In the absence of an apparatus to maintain a consistent force, measurements with no applied force may be a robust alternative when performing dose consistency measurements. This simplifies the sealant application procedure, although accurate representation of facial deposition and mask dead volume may not be realized.

It is recommended that future infant soft face model models utilize a facial backing which is manufactured as a single piece with the VeroClear throat to avoid sealing issues with putty. Advantages of the VeroClear material include translucency and impermeability. Advantages of using a hard face model include manufacturability and ease of use.

4.3 Comments on Applicability to *In Vivo* Therapeutic Aerosol Delivery

If one desires to mimic the *in vivo* situation *in vitro*, more sophisticated soft face models may be required. Hodsen *et al.* [56] measured the facial tissue thickness in healthy children as young as age 4 using an ultrasound technique. Facial tissue thickness could not be measured in infants due to a lack of bone maturity and cooperation.[56] Their study showed skin thicknesses of 1.3-6.8 mm at possible mask contact points near the nose (nasion and end of nasals), 7.1-22.1 mm at possible mask contact points near the cheeks (inferior malar, supra M^2, sub M^2, and occlusal line), and 4.6-13.3 mm at possible mask contact points below the mouth (lower lip margin, mental sulcus, and mental eminence).[56] Therefore, a thicker layer of soft facial material near the cheeks and below the mouth than above the nose seems desirable. The 5 mm thick silicone facial layer and the 8 mm thick polyurethane facial layer were within the total

range of facial tissue thickness measured by Hodsen *et al.*[56] but did not capture non-uniformity. Topical or systemic corticosteroids can induce skin atrophy leading to a thinning of the skin and can also change its mechanical properties.[57-59]

Creating a soft face model with the objective of obtaining dose estimates representative of *in vivo* data would require facial materials accurately representing the mechanical properties of human skin including its composite, anisotropic, and viscoelastic properties.[57,60] Variation in the mechanical properties of human skin is expected between age groups, genders, individuals, and the location on an individual's body.[57,60-61] Due to its viscoelasticity, skin stiffness may be a function of the time for which the mask is applied. Various instruments are discussed in Elsner *et al*.[62] for evaluating the viscoelastic parameters of human skin. Langer's lines represent the orientation of collagen fibers in the skin and different viscoelastic properties are expected when taking measurements along or across them.[60]

Serup[57] cautions against the use of an elastic modulus for modeling human skin. However, it has been suggested that Hooke's law may be applied for very low strains.[63] The elastic modulus of female skin has been shown to be higher than male skin.[58] The elastic modulus of the human forearm has been suggested to vary from 0.1-10 MPa.[64] The elastic modulus of the polyurethane used in this study is 0.12 MPa according to the manufacturer[65] and is on the lower end of this range, which is desired for an infant model since infant skin is commonly described as soft and tender.[66]

CHAPTER 4: DISCUSSION

Skin hydration plays an important role in the physical properties of the skin.[61] The elastic modulus of the stratum corneum has been suggested to decrease by a factor of 100 for an increase in relative humidity from 40% to 100%.[67]

The electrical properties of the skin are discussed by Edwards[68] and Edelberg.[69] A literature review on the relative permittivity and electrical conductivity of the human lung, muscle, fat, and skin for wet and dry conditions, as well as other organs, is given for a wide range of frequencies by Gabriel *et al.*[70]

The very soft polyurethane face model was hypothesized to be the most representative of the *in vivo* situation and was shown to produce an adequate face mask seal at 1.5 lb. However, the stickiness of the material is not representative of that on an infant's face, and slight manufacturing defects associated with molding difficulties were present. In addition, at 3.5 lb the polyurethane facial material deformed so much that the nose abutted the exhalation valve and the mouth was located very near the inhalation valve, which is not likely realistic.

In a study using the same silicone and polyurethane facial materials as used here, Golshahi *et al*.[47] showed that for N95 masks, *in vitro* face mask-fit was not representative of *ex vivo* face mask-fit, and speculated that for N95 masks the actual strains on the test subjects' faces were not simulated by these materials. Similar studies to that performed by Golshahi *et al.*[47] comparing *in vitro* and *ex vivo* face mask-fit for pharmaceutical aerosol masks may be of interest if further advancement of soft face models is desired.

CHAPTER 5: CONCLUSIONS

5.1 Study Highlights

In conclusion, the use of soft face models increased *in vitro* lung dose due to a tighter face mask seal. At 3.5 lb lung dose differed less between hard and soft face models than at 1.5 lb. Mask dead volume had little impact on the differences in lung dose between face models at the same applied force, with only a slightly greater impact on the differences in lung dose between 1.5 lb and 3.5 lb of force. Experimental measurement of Q_{VHC} was the most predictive parameter of differences in lung dose between face models and applied forces, according to the mathematical model. Increased facial deposition on the very soft polyurethane face model at 3.5 lb likely led to the lower measurement of lung dose as compared to 1.5 lb. The use of a sealant to obtain a reliable, complete seal is required when using a hard ABS or soft silicone facial material with 1.5 lb of applied force or less to ensure lung dose consistency from run to run.

5.2 Contribution to Knowledge

This study is the first to quantify the relative importance of face mask seal and mask dead volume on infant lung dose for a commonly used VHC and face mask. The use of soft facial materials was shown to increase lung dose *in vitro*, relative to hard face models without a sealant. The negligible effect of mask dead volume differences between applied forces indicated that for a given valved holding chamber, face mask seal is the most important factor in determining lung dose.

For dose consistency, both *in vitro* and *in vivo*, it is desirable to obtain a full face mask seal. This can be achieved *in vitro* using either a soft face model or a hard face model with an additional sealant.

5.3 Future Work

Future work could involve similar experiments with more pMDI, VHC, and face mask designs. Child and adult face models could also be tested. More applied forces could be tested to obtain lung dose versus applied force curves for each VHC and face mask combination with the idealized infant geometry. The effect of different facial contours and more complex face designs could be tested and patient specific breathing patterns could be used. A comparison of *ex vivo* - *in vitro* pharmaceutical aerosol face mask fit seems desirable.

BIBLIOGRAPHY

1. Geller P, and Berlinski A: Aerosol Delivery of Medication. In: American Academy of Pediatrics Section on Pediatric Pulmonlogy, (eds). *Pediatric pulmonology*. American Academy of Pediatrics, Elk Grove Village, ILL; pp.913-932, 2011.

2. Janssens HM, and Tiddens HAWM: Aerosol therapy: the special needs of young children. Paediatr Respir Rev. 2006;7S:S83-S85.

3. Allergy & Asthma Network Mothers of Asthmatics: Holding chambers and spacers. Available at URL: http://www.aanma.org/2009/03/holding-chambers-and-spacers/. Visited May 5, 2014.

4. Erzinger S, Schueepp KG, Brooks-Wildhaber J, Devadason SG, and Wildhaber JH: Facemasks and aerosol delivery *in vivo*. J Aerosol Med. 2007;20:S78-S84.

5. Esposito-Festen JE, Ates B, van Vliet FJM, Verbraak AFM, de Jongste JC, and Tiddens HAWM: Effect of facemask leak on aerosol delivery from a pMDI-spacer system. J Aerosol Med. 2004;17:1-6.

6. Smaldone GC, Berg E, and Nikander K: Variation in pediatric aerosol delivery: importance of facemask. J Aerosol Med. 2005;18:354-363.

7. Amirav I, and Newhouse MT: Deposition of small particles in the developing lung. Paediatr Respir Rev. 2012;13:73-78.

8. Janssens HM, Heijnen EMEW, de Jong VM, Hop WCJ, Holland WPJ, de Jongste JC, and Tiddens HAWM: Aerosol delivery from spacers in wheezy infants: a daily life study. Eur Respir J. 2000;16:850-856.

BIBLIOGRAPHY

9. Esposito-Festen J, Ates B, van Vliet F, Hop W, and Tiddens H: Aerosol delivery to young children by pMDI-spacer: is facemask design important? Pediatr Allergy Immunol. 2005;16:348-353.

10. Amirav I: Infant aerosol holding chamber face masks: not all are born equal! Respir Care. 2006;51:123-125.

11. Everard ML: Inhalation therapy for infants. Adv Drug Delivery Rev. 2003;55:869-878.

12. Amirav I: Elements of mask design for successful aerosol delivery. [Abstract only]. O-22. ISAM 19th International Congress. International Society for Aerosols in Medicine, Chapel Hill, NC. April 6-10, 2013.

13. Amirav I, Luder A, Chleechel A, Newhouse MT, and Gorenberg M: Lung aerosol deposition in suckling infants. Arch Dis Child. 2012;97:497-501.

14. Everard ML, Clark AR, and Milner AD: Drug delivery from holding chambers with attached facemask. Arch Dis Child. 1992;67:580-585.

15. Shah SA, Berlinski AB, and Rubin BK: Force-dependent static dead space of face masks used with holding chambers. Respir Care. 2006;51:140-144.

16. Amirav I, and Newhouse MT: Dead space variability of face masks for valved holding chambers. Isr Med Assoc J. 2008;10:224-226.

17. Chavez A, McCracken A, and Berlinski A: Effect of face mask dead volume, respiratory rate, and tidal volume on inhaled albuterol delivery. Pediatr Pulmonol. 2010;45:224-229.

18. Bisgaard H, Anhøj J, and Wildhaber JH: Spacer devices. In: Bisgaard H, O'Callaghan C, and Smaldone GC, (eds). *Drug delivery to the lung*. Marcel Dekker, Inc., New York, NY; pp.389-420, 2002.

19. Barry PW, and O'Callaghan C: The effect of delay, multiple actuations and spacer static charge on the *in vitro* delivery of budesonide form the Nebuhaler. Br J Clin Pharmacol. 1995;40:76-78.

20. Kamin W, and Ehlich H: *In vitro* comparison of output and particle size distribution of budesonide from metered-dose inhaler with three spacer devices during pediatric tidal breathing. Treat Respir Med. 2006;5:203-508.

21. O'Callaghan C, Lynch J, Cant M, and Robertson C: Improvement in sodium cromoglycate delivery from a spacer device by use of an antistatic lining, immediate inhalation, and avoiding multiple actuations of drug. Thorax. 1993;48:603-606.

22. Bisgaard H: A metal aerosol holding chamber devised for young children with asthma. Eur Respir J. 1995;8:856-860.

23. Bisgaard H, Anhøj J, Klug B, and Berg E: A non-electrostatic spacer for aerosol delivery. Arch Dis Child. 1995;73:226-230.

24. Wildhaber JH, Devadason SG, Hayden MJ, James R, Dufty AP, Fox RA, Summers QA, and LeSouëf PN: Electrostatic charge on a plastic spacer device influences the delivery of salbutamol. Eur Respir J. 1996;9:1943-1946.

25. Kenyon CJ, Thorsson L, Borgström L, and Newman SP: The effects of static charge in spacer devices on glucocorticosteroid aerosol deposition in asthmatic patients. Eur Respir J. 1998;11:606-610.

26. Wildhaber JH, Devadason SG, Eber E, Hayden MJ, Everard ML, Summers QA, and LeSouëf PN: Effect of electrostatic charge, flow, delay, and multiple actuations on the *in vitro* delivery of salbutamol from different small volume spacers for infants. Thorax. 1996;51:985-988.

27. Dewsbury NJ, Kenyon CJ, and Newman SP: The effect of handling techniques on electrostatic charge on spacer devices: a correlation with *in vitro* particle size analysis. Int J Pharm. 1996;137:261-264.

28. Lipworth BJ, Lee DKC, Anhøj J, and Bisgaard H: Effect of plastic spacer handling on salbutamol lung deposition in asthmatic children. Br J Clin Pharmacol. 2002;54:544-547.

29. Janssens HM, de Jongste JC, Fokkens WJ, Robben SGF, Wouters K, and Tiddens HAWM: The Sophia Anatomical Infant Nose-Throat (Saint) model: a valuable tool to study aerosol deposition in infants. J Aerosol Med. 2001;14:433-441.

30. Laube BL, Sharpless G, Shermer C, Nasir O, Sullivan V, and Powell K: Deposition of albuterol aerosol generated by pneumatic nebulizer in the Sophia Anatomical Infant Nose-Throat (Saint) model. Pharm Res. 2010;27:1722-1729.

31. Finlay WH: Inertial sizing of aerosol inhaled during pediatric tidal breathing from an MDI with attached holding chamber. Int J Pharm. 1998;168:147-152.

32. Janssens HM, de Jongste JC, Hop WCJ, and Tiddens HAWM: Extra-fine particles improve lung delivery of inhaled steroids in infants: a study in an upper airway model. Chest. 2003;123:2083-2088.

33. Janssens HM, van der Wiel EC, Verbraak AFM, de Jongste JC, Merkus PJFM, and Tiddens HAWM: Aerosol therapy and the fighting toddler: is administration during sleep an alternative? J Aerosol Med. 2003;16:395-400.

34. Esposito-Festen J, Ijsselstijn H, Hop W, van Vliet F, de Jongste J, and Tiddens H: Aerosol therapy by pressurized metered-dose inhaler-spacer in sleeping young children: to do or not to do? Chest. 2006;130:487-192.

35. Janssens HM, Krijgsman A, Verbraak TFM, Hop WCJ, de Jongste JC, and Tiddens HAWM: Determining factors of aerosol deposition for four pMDI-spacer combinations in an infant upper airway model. J Aerosol Med. 2004;17:51-61.

36. Everard ML: Playing the game: designing inhalers for pediatric use. In: Dalby RN, Byron PR, Peart JP, and Suman JD, (eds). *RDD Europe 2007*. Davis Healthcare International Publishing, LLC, River Grove, ILL; pp.71-78, 2007.

37. Amirav I, Mansour Y, Mandelberg A, Bar-Ilan I, and Newhouse MT: Redesigned face mask improves “real life” aerosol delivery for Nebuchamber. Pediatr Pulmonol. 2004;37:172-177.

38. Louca E, Leung K, Coates AL, Mitchell JP, and Nagel MW: Comparison of three valved holding chambers for the delivery of fluticasone propionate-HFA to an infant face model. J Aerosol Med. 2006;19:160-167.

39. Laube BL, Sharpless G, Harrand V, Zinreich J, Sedberry K, Przekwas A, Knaus D, Barry J, and Papania M: Intranasal deposition of liquid aerosol in anatomically-correct models of 2, 5 and 12 year-old children. [Abstract only]. P-084. ISAM 18th International Congress. International Society for Aerosols in Medicine, Rotterdam, Netherlands. June 18-22, 2011.

40. Liberman EA, Sousa NM, and von Hollen D: *In vitro* techniques for evaluating eye deposition of aerosolized drug associated with nebulizer facemasks. In: Dalby RN, Byron PR, Peart JP, Suman JD, Farr SJ, and Young PM, (eds). *RDD 2008*. Davis Healthcare International Publishing, LLC, River Grove, ILL; pp.731-734, 2008.

41. Mitchell JP, Wiersema KJ, MacKay HA, Nagel MW, Pischel SM, and Cripps AL: Novel approach for evaluating medication delivered via valved holding chambers (VHCs) with facemask using a face model for infants and small children. In: Dalby RN, Byron PR, Peart JP, Suman JD, Farr SJ, and Young PM, (eds). *RDD 2008*. Davis Healthcare International Publishing, LLC, River Grove, ILL; pp.785-788, 2008.

42. Hsu W, Bai T, von Hollen D, Nikander K, and Dalby R: Realistic evaluation of a valved holding chamber with facemask – using a soft anatomical model face to evaluate aerosol output under simulated conditions. In: Dalby RN, Byron PR, Peart JP, Suman JD, Farr SJ, and Young PM, (eds). *RDD 2010*. Davis Healthcare International Publishing, LLC, River Grove, ILL; pp.835-838, 2010.

43. Xu Z, Hsu W, von Hollen D, Viswanath A, Nikander K, and Dalby R: Delivery efficiency from valved holding chambers with facemasks: a comparative study using soft anatomical models. In: Dalby RN, Byron PR, Peart JP, Suman JD, Farr SJ, and Young PM, (eds). *RDD 2012*. Davis Healthcare International Publishing, LLC, River Grove, ILL; pp.809-813, 2012.

44. Mitchell JP, Finlay JB, Nutall JM, Limbrick MR, Nagel MW, Avvakoumova VI, MacKay HA, Ali RS, and Doyle CC: Validation of a new model infant face with nasopharynx for the testing of valved holding chambers (VHCs) with facemask as a patient interface. In: Dalby RN, Byron PR, Peart JP, Suman JD, Farr SJ, and Young PM, (eds). *RDD 2010*. Davis Healthcare International Publishing, LLC, River Grove, ILL; pp.777-780, 2010.

45. Mitchell J, and Dolovich MB: Clinically relevant test methods to establish *in vitro* equivalence for spacers and valved holding chambers used with pressurized metered dose inhalers (pMDIs). J Aerosol Med Pulm Drug Deliv. 2012;25:217-242.

46. Mitchell JP: Appropriate face models for evaluating drug delivery in the laboratory: the current situation and prospects for future advances. J Aerosol Med Pulm Drug Deliv. 2008;21:97-111.

47. Golshahi L, Telidetzki K, King B, Shaw D, and Finlay WH: A pilot study on the use of geometrically accurate face models to replicate *ex vivo* N95 mask fit. Am J Infect Control. 2013;41:77-79.

48. Javaheri E, Golshahi L, and Finlay WH: An idealized geometry that mimics average infant nasal airway deposition. J Aerosol Sci. 2013;55:137-148.

49. Storey-Bishoff J, Noga M, and Finlay WH: Deposition of micrometer-sized aerosol particles in infant nasal airway replicas. J Aerosol Sci. 2008;39:1055-1065.

50. EXSEAL Corporation: Product lineup. *EXSEAL Corporation*. Available at URL: http://www.exseal.net/details.html#07. Visited February 27, 2013.

51. Trudell Medical International: AeroChamber Plus with Flow-Vu Valved Holding Chamber Product Monograph. *Trudell Medical International*. Available at URL: http://www.trudellmed.com/sites/trudellmed.com/files/pdf/consumer/ACIFI_ProdMono.pdf. Visited March 27, 2013.

52. Mainline Medical: Vital Signs Marquest Respirgard-II 303 Bacterial Filter. Available at URL: http://www.mainlinemedical.com/mm/vital-signs-marquest-respirgard-ii-303-bacterial-filter.html. Visited April 15, 2014.

53. Canadian Standards Association: Spacers and holding chambers for use with metered-dose inhalers. Mississauga, ON, Canada. CAN/CSA/Z264.1-02: 2002 (R 2011). *Canadian Standards Association*. Available at URL: http://shop.csa.ca/en/canada/drug-labeling-and-delivery/cancsa-z2641-02-r2011/invt/27017422002. Visited March 27, 2013.

54. Berg E, Madsen J, and Bisgaard H: *In vitro* performance of three combinations of spacers and pressurized metered dose inhalers for treatment in children. Eur Respir J. 1998;12:472-476.

55. Zak M, Madsen J, Berg E, Bülow J, and Bisgaard H: A mathematical model of aerosol holding chambers. J Aerosol Med. 1999;12:187-196.

56. Hodsen G, Lieberman LS, and Wright P: In vivo measurements of facial tissue thicknesses in American Caucasoid children. J Forensic Sci. 1985;30:1100-1112.

57. Serup J: Mechanical properties of human skin: elasticity parameters and their relevance. In: Elsner P, Berardesca E, Wilhelm K-P, and Maibach HI, (eds). *Bioengineering of the skin: skin biomechanics*. CRC Press, Boca Raton, FL; pp.41-48, 2002.

58. Oikarinen A, and Knuutinen A: Mechanics of human skin: biochemical aspects. In: Elsner P, Berardesca E, Wilhelm K-P, and Maibach HI, (eds). *Bioengineering of the skin: skin biomechanics*. CRC Press, Boca Raton, FL; pp.3-16, 2002.

59. Vogel HG: Mechanical properties of human skin: animal models. In: Elsner P, Berardesca E, Wilhelm K-P, and Maibach HI, (eds). *Bioengineering of the skin: skin biomechanics*. CRC Press, Boca Raton, FL; pp.17-40, 2002.

60. Wright K: Elasticity and deformation of skin. In: Elden HR, (eds). *Biophysical properties of the skin*. Wiley-Interscience, New York, NY; pp.437-449, 1971.

61. Larsen TH, and Jemec GBE: Skin mechanics and hydration. In: Elsner P, Berardesca E, Wilhelm K-P, and Maibach HI, (eds). *Bioengineering of the skin: skin biomechanics*. CRC Press, Boca Raton, FL; pp.199-206, 2002.

62. Elsner P, Berardesca E, Wilhelm K-P, and Maibach HI. *Bioengineering of the skin: skin biomechanics*. CRC Press, Boca Raton, FL; pp. 63-178, 2002.

63. Daly CH, and Odland GF: Age-related changes in the mechanical properties of human skin. J Invest Dermatol. 1979;73:84-87.

64. Zahouani H, Asserin J, and Humbert P: Mechanical properties of the human skin during friction assessment. In: Elsner P, Berardesca E, Wilhelm K-P, and Maibach HI (eds). *Bioengineering of the skin: skin biomechanics*. CRC Press, Boca Raton, FL; pp.49-58, 2002.

65. EXSEAL Corporation: Urethane gel physical property data. *EXSEAL Corporation*. Available at URL: http://www.exseal.net/data.html. Visited April 21, 2014.

66. Stamatas GN, Nikolovski J, Luedtke MA, Kollias N, and Wiegand BC: Infant skin microstructure assessed in vivo differs from adult skin in organization and at the cellular level. Pediatr Dermatol. 2010;27:125-131.

67. Lévêque J-L, and Rasseneur L: Mechanical properties of stratum corneum: influence of water and lipids. In: Marks R, Barton SP, and Edwards C, (eds). *The physical nature of the skin*. MTP Press, Lancaster, England; pp.155-161, 1988.

68. Edwards C: The electrical properties of skin. In: Marks R, Barton SP, and Edwards C, (eds). *The physical nature of the skin*. MTP Press, Lancaster, England; pp.209-213, 1988.

69. Edelberg R: Electrical properties of skin. In: Elden HR, (eds). *Biophysical properties of the skin*. Wiley-Interscience, New York, NY; pp.513-550, 1971.

70. Gabriel C, Gabriel S, and Corthout E: The dielectric properties of biological tissues: I. Literature survey. Phys Med Biol. 1996;41:2231-2249.

APPENDIX A

The following is a sample calculation using the mathematical lung dose model applied to the average results of measurements with the ABS face model at 3.5 lb of applied force.

Substituting equation (2) into equation (1) gives the volume of aerosol reaching the lungs, V_a, as:

$$V_a = Q_{VHC} * t_i - a * MDV - b * V_{NA}$$

where Q_{VHC}=2.32 l min^{-1} is the volume flow rate through the VHC as given in Table 2, t_i=0.65 s is the measured inspiration time as per Section 2.9, a=0.1 is the fraction of the MDV inhaled as per Section 2.10, MDV=14.8 ml is the measured mask dead volume as given in Table 1, b=0.9 is the fraction of the nasal airway dead volume inhaled as per Section 2.10, and V_{NA} is the nasal airway volume of 11.4 ml as per Section 2.1. Converting to consistent units and substituting in these values:

$$V_a = 38.\bar{6}\ ml\ s^{-1} * 0.65\ s - 0.1 * 14.8\ ml - 0.9 * 11.4ml = 13.4\ ml$$

Substituting equation (4) into equation (3) gives the lung dose for the first breath as:

$$LD_1 = V_a * \frac{ED * DD}{V_{VHC}} * (1 - \eta)$$

where V_a has just been solved, ED is the fraction of the delivered dose, DD, initially available for inhalation from the VHC taken as 0.27 as per Section 2.10, DD=80.4 µg as per Section 3.4, V_{VHC}=149 ml is the volume of the VHC as per section 2.10, and η =0.024 is the nasal deposition fraction based on interpolation of the first two rows in Table 2 of Javaheri *et al.*[48] for an aerodynamic diameter of 1.1 µm. Solving:

$$LD_1 = 13.4\,ml * \frac{0.27 * 80.4\,\mu g}{149\,ml} * (1 - 0.024) = 1.9\,\mu g$$

Substituting equation (2) into equation (5) gives the remaining fraction of aerosol in the VHC after one breath, RF, as:

$$RF = \left[1 - \frac{Q_{VHC} * t_i}{V_{VHC}}\right] e^{\frac{\ln(1/2)}{T_{1/2} f}}$$

where $T_{1/2}$ is the aerosol half-life in the antistatic VHC taken as 30 seconds as per Section 2.10, and f=0.48 s^{-1} is the respiratory cycle breathing frequency as per Section 2.10. Solving:

$$RF = \left[1 - \frac{(38.\overline{6}\,ml\,s^{-1}) * (0.65\,s)}{(149\,ml)}\right] * e^{\frac{-0.693}{(30\,s)*(0.48\,s^{-1})}} = 0.792$$

Equation (7) gives the total lung dose as:

$$LD = LD_1 * \frac{1 - RF^n}{1 - RF}$$

where n is the number of respiratory cycles equal to 6 in this study as per Section 2.9, and LD_1 and RF have been previously calculated. Solving:

$$LD = 1.9\,\mu g * \frac{1 - 0.792^6}{1 - 0.792} = 6.9\,\mu g$$

This result is seen in Figure 13. Calculations for the other face models and applied forces are similar, with MDV and Q_{VHC} being the only variables to change based on Table 1 and Table 2, respectively.